

# A98-31503

## ACCURACY OF UNSTEADY TRANSONIC FLOW COMPUTATIONS

ICAS-98-2,4,2

T. A. Grønland\*, P. Eliasson‡ and J. Nordström†  
FFA, The Aeronautical Research Institute of Sweden  
Bromma, SWEDEN

### Abstract

In this work we will discuss the accuracy one can obtain in predictions of unsteady transonic flows by a modern CFD method, in this case a time accurate Reynolds-averaged Navier-Stokes solver.

The test case used in this study is an 18% thick biconvex, two-dimensional airfoil. Experiments have revealed that this geometry shows a strong oscillatory flow in a certain Mach number regime, often referred to as buffet.

Sensitivity to numerical and physical modeling is assessed through repeated computations with various spatial and temporal discretization, numerical schemes and different types of turbulence models. The correlation between the airfoil in a free flight- and in a wind-tunnel environment is also investigated.

It is shown that modern CFD methods can indeed predict the complex buffet phenomena with reasonable accuracy. This work highlights some of the most critical aspects of physical and numerical modeling of buffet. It is also shown that lift and drag on the airfoil differs considerably between the free flight- and wind tunnel environments.

### 1 Nomenclature

CFD	Computational Fluid Dynamics
$C_L$	Lift coefficient [-]
$C_D$	Drag coefficient [-]
T	Time [s]
c	Airfoil chord [m]
U	Velocity [m/s]
$\omega$	Frequency [rad/s]
k	Reduced frequency [-], $k = \omega c / 2U_\infty$
$y^+$	Viscous wall unit [-]

#### Subscripts

$\infty$  Free stream, infinity

\* Research Scientist, present address: Prosovia Research & Technology, Stockholm, Sweden.

‡ Research Scientist

† Senior Scientist

### 2 Introduction

Turbulent high Reynolds number flows have for many years been a challenge for the CFD community. Test cases with separated flow (e.g. shock induced) are commonly used for code validation purposes. In the past few years, time accurate CFD methods for unsteady flows have become very popular and widely spread.

To validate time accurate CFD methods for most practical applications, means high Reynolds number turbulent flow calculations. Add to this the complexity of shock-boundary layer interaction and shock-induced separation, and the result is transonic buffet, a very intricate validation case.

The buffet phenomenon is mainly characterized by the frequency and amplitude of lift and drag on the airfoil. Hence the capability of predicting the buffet frequency and amplitude accurately is focused upon in this study.

Buffet or buffeting (where also the structure is involved) are self-excited unsteady flow phenomena with several important practical applications. E.g. on a transport aircraft, onset of buffet, and later buffeting, might be the limiting factor for the aircraft's cruise Mach number. For a fighter aircraft, buffeting phenomena might limit the target track capabilities of wing mounted weapons. So indeed there is a need for accurate, unsteady simulation capabilities.

### 3 CFD Methodology

#### 3.1 Description of the EURANUS code

EURANUS<sup>1,4,5</sup> is a general three-dimensional code that solves the time dependent Euler or Reynolds averaged Navier-Stokes equations on a structured multi-block mesh utilizing a cell centered finite volume formulation.

A large variety of physical models and numerical methods are implemented. The physical modeling cov-

ers the range from calorically perfect gas to gas in thermal and chemical non-equilibrium. Available types of turbulence models are various algebraic, two-equation or Reynolds stress models.

Different discretization schemes are, e.g. central differences with artificial dissipation or upwind schemes with TVD or flux vector splitting. A variety of temporal discretization schemes, explicit or implicit, are available. In this work an implicit time accurate method<sup>4,6,7</sup> is used. Various convergence acceleration methods, such as multigrid and residual smoothing, are available.

### 3.2 Description of computational mesh

The computational grids used here are of the so called C-type. They typically have 128 cells around the airfoil and 64 cells in the wall normal direction plus additional cells in the wake. The first layer of cells is placed above the surface in such a way that the viscous wall unit,  $y^+$ , is near unity, which indicates that the boundary layer is properly resolved.

Two different grids are created using the grid generation tool FFANET<sup>2</sup>, one for the airfoil in a free flight configuration with the external (artificial) boundaries located more than 20 chords away from the profile, and another grid in a wind tunnel like configuration with the external boundaries fitted to the geometry of the test section from the NASA Ames tunnel used by McDevitt<sup>3</sup> et. al.

Close-ups of the free flight configuration, and the entire wind tunnel configuration meshes are shown in Figures 1 and 2 respectively.

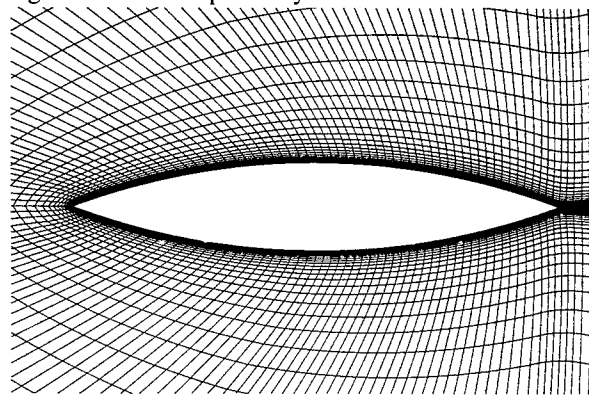


Fig. 1: Close-up of the grid near the profile (free flight configuration).

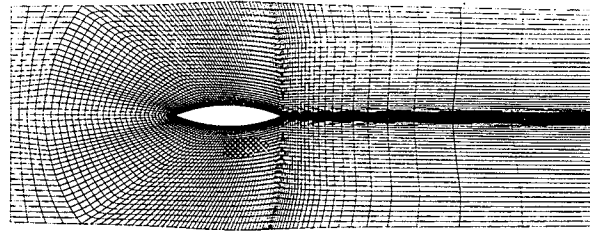


Fig. 2: Grid and computational domain for the wind tunnel configuration.

The grids shown here are used for the bulk of the CFD analysis. However, additional grids, obtained by doubling and reducing the number of cells by a factor 4, were used to check for grid convergence.

### 4 General flow features

A general view of the flow in the free flight environment is given by the instantaneous Mach number plots in Figure 3. The free stream Mach number is 0.783 and the Reynolds number  $11 \cdot 10^6$ . Red (dark) color indicates supersonic flow);

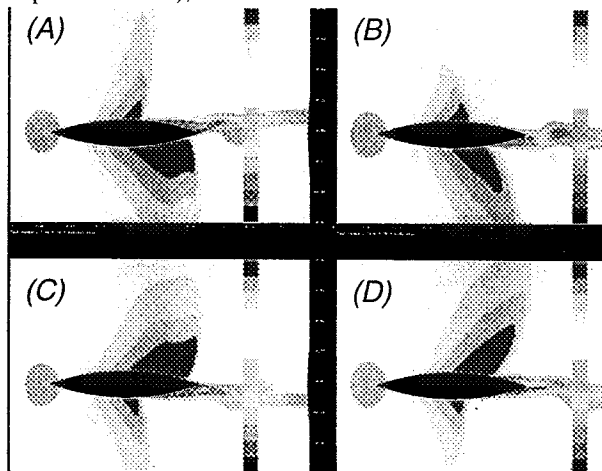


Fig. 3: Instantaneous Mach number distribution at (A) time  $T=2.5$  ms, near minimum  $C_L$ , (B) time  $T=8.75$  ms, near  $C_L=0$  and increasing, (C) time  $T=16.25$  ms, near maximum  $C_L$  and (D) time  $T=22.0$  ms, near  $C_L=0$  and decreasing.

Note particularly the Mach number fields at  $T=8.75$  ms and at  $T=22.0$  ms, which both are taken at zero lift. These plots clearly shows the hysteresis effects in buffet.

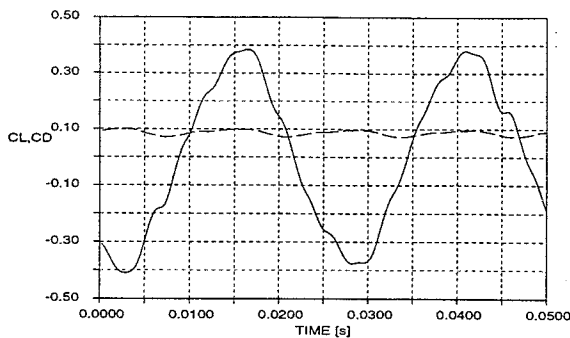


Fig. 4: Lift and drag coefficient as function of time.

In Figure 4 it is seen that both lift and drag on the profile show a periodic oscillation with a reduced frequency of approximately 0.44. Both the lift and drag curves seem to consist of several small amplitude, high frequency modes superimposed on the fundamental.

We compare the CFD results with the measurements by McDevitt<sup>3</sup>. We focus the investigation on predicted frequency and amplitude of lift and drag. No experimental instantaneous pressure distributions were reported<sup>3</sup>.

### 5 Sensitivity to physical and numerical modeling, free flight environment

This section is focused on buffet in a free flight environment. The free stream Mach number is 0.783 and the Reynolds number  $11 \cdot 10^6$ . The objective is to investigate the sensitivity from different physical and numerical modeling.

#### 5.1 Spatial resolution

To check for grid convergence, we repeat the computation on three different grids, with approximately 49000, 12000 and 3000 cells in a two-dimensional plane. In Figure 5 the lift coefficient is shown as function of time from computations done on the three meshes.

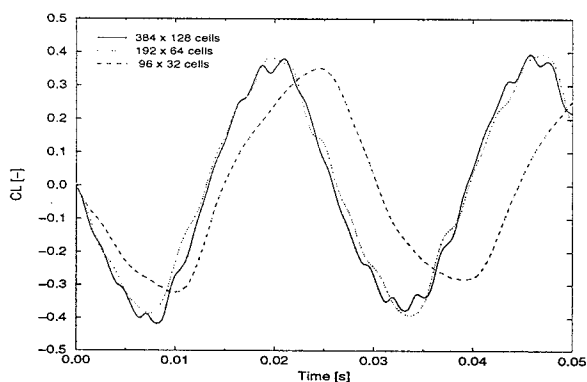


Fig. 5: Lift as function of time on three different grids.

Both the amplitude and the frequency are only slightly influenced by the spatial resolution as long as at least 192 by 64 cells are used. Note that the 384 by 128 cell grid appears to resolve some small amplitude, high frequency modes which are superimposed on the fundamental. However, this does not influence either the frequency nor the amplitude of the fundamental.

Using the 192 by 64 cells grid together with a time step of 0.25 ms, a second order upwind scheme and an algebraic turbulence model will hereafter be referred to as the 'baseline' computation around which the variations in numerical and physical modeling are done. Finally we remark here that the CPU time increases with roughly a factor 10 between each of the three grids.

#### 5.2 Temporal resolution

To investigate the sensitivity of the predicted lift coefficient to temporal resolution, a number of simulations were performed using time steps between 0.125 and 4.0 ms.

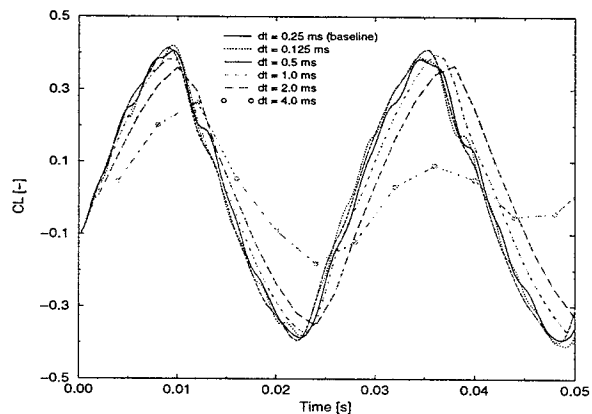


Fig. 6: Lift as function of time for various temporal resolutions.

Figure 6 shows that an appropriate time step is 0.5 ms or smaller, which corresponds to approximately 50 iterations, or more, per cycle.

#### 5.3 Spatial discretization schemes

Two popular classes of spatial discretization schemes are central difference and different upwind schemes. The major difference lies in the capability of handling discontinuities (shocks). In this work, three different schemes are considered; A second order central difference scheme, a first and a second order upwind scheme. The lift coefficient as function of time from computations using the different schemes is shown in Figure 7.

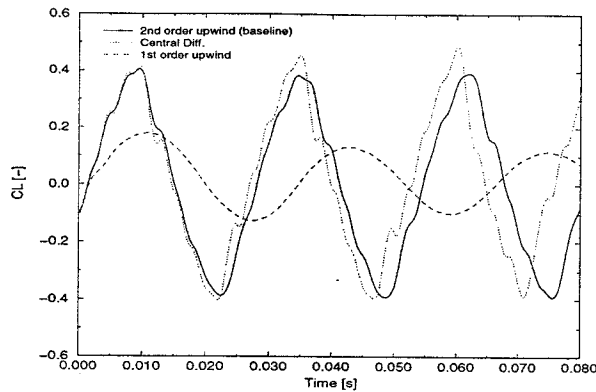


Fig. 7: Lift as function of time for various spatial discretization schemes.

Substantial differences in both frequency and amplitude are obtained with the three different schemes. The first order upwind scheme obviously damps the amplitude and lowers the frequency. This scheme is simply not accurate enough and hence should not be regarded as appropriate for this type of flow.

Surprisingly, there is also a significant difference between the two second order accurate schemes. In terms of reduced frequency, the numbers are 0.44 for the 2nd order upwind scheme and 0.46 for the central difference scheme.

#### 5.4 Turbulence modeling

Modeling of turbulence is an important issue when solving the Reynolds-averaged Navier-Stokes equations. Here we compare the solution obtained with two different turbulence models, namely the algebraic Baldwin-Lomax<sup>12</sup> model and the two-equation k-ε model of Chien<sup>13</sup>.

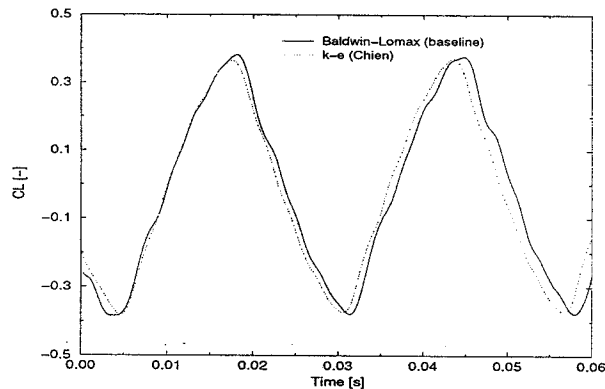


Fig. 8: Lift as function of time for the two different turbulence models.

These two turbulence models represent two different classes of models with considerable differences in capability of handling e.g. history effects and separated

flows. The results obtained here indicate that turbulence modeling influences the predicted frequency significantly. In this case, the reduced frequency changes from 0.44 for the Baldwin-Lomax model to nearly 0.46 for Chien k-ε model.

#### 6 Simulated wind tunnel environment

This section is focused on buffet in a wind tunnel environment. The free stream Mach number is 0.754 and the Reynolds number is  $11 \cdot 10^6$ . The static pressure is prescribed at the exit tunnel boundary such that the correct Mach number is obtained. The objective is to find the correlations, in terms of frequency and amplitude, between the free flight and wind tunnel environments.

Before we proceed, note that we compare a Mach 0.754 wind tunnel case with a Mach 0.783 free flight case. The reason being that the Mach number range where buffet occurs is shifted towards a lower Mach number in the wind tunnel environment. This shift in buffet Mach number makes the comparison between the two cases somewhat difficult, but not less important. The comparison will also show the difficulty of wind tunnel to free flight extrapolation for buffet phenomena.

A general view of the flow is given in Figure 9 by the instantaneous Mach number plots. (see also Figure 10 for reference). Red (dark) color indicates supersonic flow);

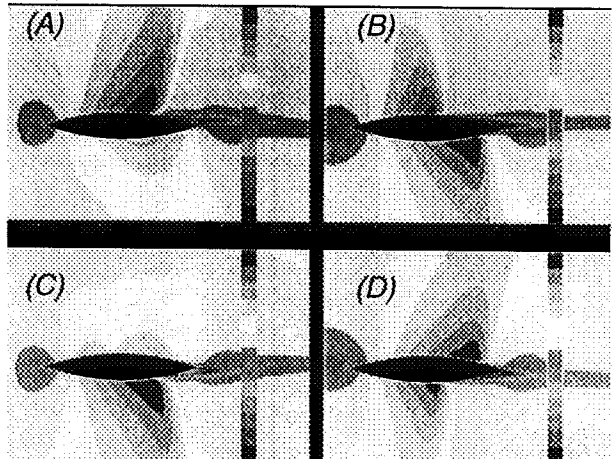


Fig. 9: Instantaneous Mach number distribution at (A) time  $T=0$  ms, near minimum  $C_L$ , (B) time  $T=7$  ms, (C) time  $T=14$  ms, near maximum  $C_L$  and (D) time  $T=21$  ms.

The Mach number fields in Figure 9 are shown at approximately the same points in the cycle as for the Mach number fields in Figure 3.

In Figure 10 lift and drag is shown as function of time.

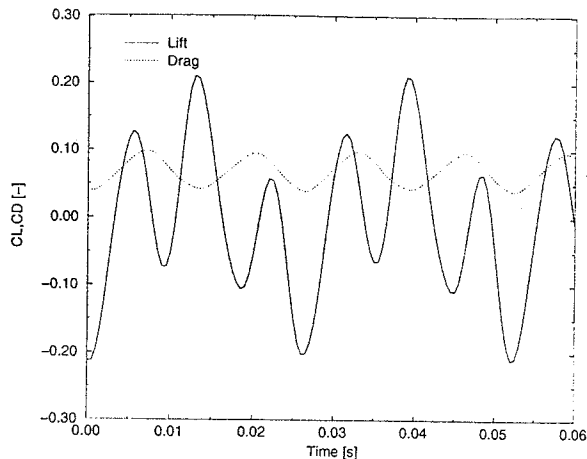


Fig. 10: Lift and drag coefficient as function of time.

Both lift and drag show a periodic oscillation with a reduced frequency of about 0.47. However, compared with the corresponding plot for the free flight environment (see Figure 4), a dramatic difference in  $C_L$  through the cycle is found. In the wind tunnel case,  $C_L$  changes sign 6 times compared to 2 times in the free flight situation.

Note also that the reduced frequency of 0.47 differs significantly from 0.44, obtained in the free flight case with the same physical and numerical modeling.

### 7 Other effects

In sections 5 and 6 we have shown how the CFD results are influenced by some aspects of physical and numerical modeling as well as the presence of wind tunnel walls. However, there are, of course, other effects which might influence the accuracy of the results presented here.

Examples of effects which are excluded in this study are: Three dimensionality of the flow, transition to turbulence and the influence of boundary conditions. Other aspects such as temporal discretization schemes, convergence strategies, etc. are covered elsewhere<sup>4,5</sup>.

### 8 Summary and Conclusions

Transonic buffet on the 18% biconvex airfoil has previously been investigated both experimentally and by numerical methods<sup>3,8,9,10,11</sup>. In the experiments a reduced frequency of 0.49 is reported. In the present study a frequency of 0.47 is found for the wind tunnel simulation, while 0.44 was obtained for the free flight environment (both using the baseline modeling, see Section 5.1). In other computational studies, frequencies of 0.40, 0.41 and 0.43 are reported for the free flight case

In the free flight case, frequencies in the range 0.44 to 0.48 are found, depending primarily on the choice of spatial discretization scheme and turbulence model.

From the present work we conclude that;

- Turbulence modeling and spatial discretization schemes are the critical issues for a CFD prediction of the buffet phenomenon.
- Significant differences between buffet in the wind tunnel and the free flight environments are observed.
- Transonic buffet can be computed with good accuracy provided that the issues above are properly handled.

### 9 References

- <sup>1</sup>Rizzi, A., Eliasson, P., Lindblad, I., Hirsch, C., Lacor, C. & Häuser, J., "The Engineering of Multiblock/Multigrid Software for Navier-Stokes Flows on Structured Meshes", *Computers Fluids*, Vol. 22, No. 2/3, pp. 341-367, 1993.
- <sup>2</sup>Tysell, L. G. & Hedman, S. G., "Towards a General Three-Dimensional Grid Generation System", ICAS-88-4.7.4, 1988.
- <sup>3</sup>Mc Devitt, J. B., Levy, L. L., Deiwert, G., "Transonic Flow about a Thick Circular-Arc Airfoil", *AIAA Journal*, Vol. 14, No. 5, May 1976.
- <sup>4</sup>Eliasson, P., Nordström, J., "The Development of an Unsteady Solver for Moving Meshes", FFA TN 1995-39
- <sup>5</sup>Eliasson, P., Nordström, J., Torngren, L., Tysell, L., Karlsson, A., Winzell, B., "Computations and Measurements of Unsteady Pressure on a Delta Wing with an Oscillating Flap", ECCOMAS 1996.
- <sup>6</sup>Jameson, A., "Time Dependent Calculations using Multigrid, with Applications to Unsteady Flows Past Airfoils and Wings", AIAA-91-1596.
- <sup>7</sup>Arnore, A., Liou, M., Povinelli, L. "Multigrid Time Accurate Integration of Navier-Stokes Equations", NASA TM 106373.
- <sup>8</sup>Edwards, J. W., Thomas, J. L., "Computational Methods for Unsteady Transonic Flows", *Unsteady Transonic Aerodynamics*, edited by David Nixon, Vol. 120 in series Progress in Astronautics and Aeronautics, 1989.
- <sup>9</sup>Steger, J. L., "Implicit Finite-Difference Simulation of Flow about Arbitrary Two-dimensional Geometries", *AIAA Journal*, Vol. 16, No. 7, July 1978.
- <sup>10</sup>Hoffren, J., "Time-Accurate Schemes for a Multi-Block Navier-Stokes Solver", Report No. A-14, Series A, Helsinki University of Technology, 1992.
- <sup>11</sup>Levy, L. L., "Experimental and Computational Steady and Unsteady Transonic Flows about a Thick Airfoil", *AIAA Journal*, Vol. 16, No. 6, June 1978.
- <sup>12</sup>Baldwin, B. S., Lomax, H., "Thin Layer Approximation and Algebraic Model for Separated Turbulent Flows", AIAA-78-257, January 1978.
- <sup>13</sup>Chien, K. Y., "Predictions of Channel and Boundary-Layer Flows with a Low-Reynolds-Number Turbulence Model", *AIAA Journal*, Vol. 20, No. 1, January, 1982.